Interferometry with relativistic electrons

K.-P. Marzlin[1,2] and T. Lee[1]
[1]*Department of Physics, St. Francis Xavier University, Antigonish, Nova Scotia B2G 2W5, Canada*
[2]*Institute for Quantum Information Science, University of Calgary, Calgary, Alberta T2N 1N4, Canada*
(Received 4 September 2013; revised manuscript received 29 April 2014; published 4 June 2014)

We propose an experiment to test the influence of Lorentz contraction on the interference pattern of a beam of electrons. The electron beam is split and recombined by two pairs of bichromatic laser pulses, using a variation of the Kapitza-Dirac effect. Between the pairs, the electrons are accelerated to relativistic speed. We show that Lorentz contraction of the distance between two partial beams will then lead to a reduction of fringe visibility. The connection of the proposal to Bell's spaceship paradox is discussed.

DOI: 10.1103/PhysRevA.89.062103 PACS number(s): 03.30.+p, 03.75.−b, 41.75.Ht

I. INTRODUCTION

The influence of special relativity on matter-wave interference is a long-established fact. For instance, the spatial interference pattern of atom interferometers that are based on optical Ramsey fringes [1] can only be fully explained if the relativistic Doppler effect is taken into account [2]. This effect is relevant even for nonrelativistic velocities because the fringe pattern is very sensitive to differences between the dynamical phase factors $\exp(-iEt/\hbar)$ of different partial beams in the interferometer. The relativistic Doppler effect essentially takes into account time dilation in the dynamical phase.

On the other hand, the consequences of Lorentz contraction in matter-wave interference are much more difficult to detect. Lorentz contraction generally has only been confirmed indirectly, for instance through the compressed charge distribution in high-energy ion collisions [3] and the wavelength of free-electron lasers [4]. The Michelson-Morley experiment, which was the reason for the introduction of Lorentz contraction, may also be considered as an indirect confirmation. An overview about experimental tests of Lorentz contraction can be found in Ref. [5].

In this paper, we suggest an experiment to observe the impact of Lorentz contraction on the spatial interference pattern of an electron interferometer. The principle idea of the proposal is that an electron beam is split, accelerated to relativistic speed, and then recombined. Lorentz contraction of the distance between two partial beams will then lead to a reduction of fringe visibility. In Sec. II, we will outline how to realize this scheme using a modification of the Kapitza-Dirac effect. A theoretical analysis of the interference pattern based on the Dirac equation in Sec. III is followed by an analysis of the beam-splitting process in Sec. IV. Numerical results for the interference pattern are presented in Sec. V, and in Sec. VI the connection of the proposal to Bell's spaceship paradox is discussed.

II. SKETCH OF PROPOSED EXPERIMENT

Our proposal employs the general principles of Ramsey-Bordé interferometers [1,6–8], in which an atomic beam is split and recombined by a sequence of laser pulses. When passing through a laser pulse, the atoms absorb photons so that momentum is transferred from the pulse to the atoms. This change in the atomic center-of-mass dynamics can be used to construct atom beam splitters. In a similar way, the Kapitza-Dirac effect [9–12] can be used to transfer momentum from a standing light wave to electrons. A Ramsey-Bordé interferometer for (nonrelativistic) electrons that employs bichromatic laser pulses as beam splitters has been described in Ref. [13]. Our proposal builds on this work.

A sketch of the suggested experiment is shown in Fig. 1(a). An electron beam initially moves in the x direction and is then coherently split into two beams, A and B, that are spatially separated by a distance Δz. The splitting is accomplished by two bichromatic laser pulses, which are represented as dashed vertical red lines in Fig. 1(a). The first pulse (leftmost dashed line) splits the electron beam into two partial beams and transfers momentum to one of the beams, thus changing their relative velocity Δv. Between the first two pulses, electrons travel freely for a time T so that they acquire a distance $\Delta z = T\Delta v$. The second laser pulse reverses the momentum transfer so that beams A and B have the same momentum.

The split electron beam then enters a region with a strong electric field that accelerates it in the z direction for a time T'. After the electrons have passed through the electric field and obtained a relativistic speed $v = \beta c$, the electrons are recombined in such a way that the spatial distance between the two beams is reduced by an amount Δz in their rest frame. For nonrelativistic electrons, this would lead to a perfect overlap, resulting in an interference pattern with high fringe visibility, but, at relativistic speed, Lorentz contraction changes this conclusion.

To understand this, consider the space-time diagram of the interferometer in Fig. 1(b), which shows that in the laboratory frame, the distance between beams A and B remains unchanged during the acceleration. However, once the electrons are moving at speed v, the proper distance $\Delta z'$ in their rest frame has to be measured simultaneously in that frame, i.e., along the lower red dashed line in Fig. 1(b) (see also Sec. VI). We then have $\Delta z' = \gamma\Delta z > \Delta z$, where $\gamma = 1/\sqrt{1-\beta^2}$, because Δz is the Lorentz contraction of $\Delta z'$. Consequently, after the recombination, beams A and B would miss each other by a distance $\Delta z' - \Delta z = (\gamma - 1)\Delta z$, which would lead to reduced fringe visibility.

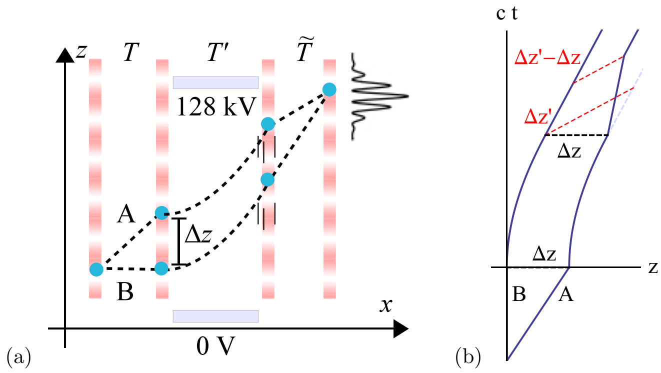

FIG. 1. (Color online) (a) Sketch of the proposed experiment. An electron beam is split and recombined using four bichromatic laser pulses and accelerated to relativistic speed. Lorentz contraction of the beam separation reduces fringe visibility. (b) Space-time diagram of the split electron beam.

III. THEORETICAL ANALYSIS OF THE INTERFEROMETER

To estimate the achievable magnitude of the beam separation, $\Delta z' - \Delta z$, we extend the description of a Ramsey-Bordé interferometer for electrons [13] to the relativistic regime. It is assumed that the beam intensity is low enough so that space-charge effects can be neglected [14]. We first summarize the key points of the nonrelativistic description.

(i) The initial electron state is expanded in terms of momentum eigenstates $\phi_p(z)$ as

$$\psi_{\text{init}}(z) = \int dp\, \tilde{\psi}(p)\phi_p(z). \tag{1}$$

It is sufficient to describe the motion along the z axis because all forces point along this direction. We consider states for which $\tilde{\psi}(p)$ is negligible if not $|p| \ll \hbar k_L$, with k_L the wave number of the laser pulses.

(ii) The free evolution of the electrons for a time T between two laser pulses amounts to the replacement of $\tilde{\psi}(p)$ by $\exp[-iTE(p)/\hbar]\,\tilde{\psi}(p)$, where $E(p)$ is the energy of an electron with momentum p.

(iii) Acceleration for a time T' amounts to a unitary transformation $\hat{U}_a(T')$ of the form

$$\hat{U}_a(T')\phi_p(z) = e^{-i\tau(p)}\,\phi_{p+maT'}(z), \tag{2}$$

$$\tau(p) = \frac{1}{\hbar}\int_0^{T'} dt'\, E(p + mat'). \tag{3}$$

(iv) The first and second laser pulses induce a unitary transformation,

$$\hat{U}_-\phi_p(z) = \frac{1}{\sqrt{2}}[\phi_p(z) + \phi_{p+2\hbar k_L}(z)], \tag{4}$$

$$\hat{U}_-\phi_{p+2\hbar k_L}(z) = \frac{1}{\sqrt{2}}[-\phi_p(z) + \phi_{p-2\hbar k_L}(z)]. \tag{5}$$

The last two laser pulses produce a similar unitary transformation $\hat{U}_+$, which is equal to $\hat{U}_-$ with k_L replaced by $-\tilde{k}_L$. These transformations are not accurate but provide a reasonable approximation for nonrelativistic electrons. We will give a detailed description of the splitting process below.

(v) Using points (i)–(iv), the electron state after passing through the interferometer evaluates to [13]

$$\begin{aligned}\psi_{\text{final}}(z) = &\frac{1}{4}\int dp\, \tilde{\psi}(p)\phi_{p+maT'}(z)\\ &\times e^{-i\tau(p,T')}[e^{-\frac{iT}{\hbar}E(p+2\hbar k_L)}e^{-\frac{i\tilde{T}}{\hbar}E(p-2\hbar\gamma\tilde{k}_L+maT')}\\ &+ e^{-\frac{iT}{\hbar}E(p)}e^{-\frac{i\tilde{T}}{\hbar}E(p+maT')}] + \text{rest}.\end{aligned} \tag{6}$$

The first term in parentheses corresponds to beam A in Fig. 1(a), i.e., to electrons which receive momentum transfers $2\hbar k_L$, $-2\hbar k_L$, $-2\hbar\tilde{k}_L$, $2\hbar\tilde{k}_L$ at the four laser pulses. The second term in parentheses corresponds to beam B, with electrons that travel through the laser pulses without changing their momentum. "Rest" refers to (seven) other partial beams that are produced in addition to beams A and B. For brevity, these beams will only be included in the numerical analysis given below.

We now adapt this derivation to relativistic electrons described by the Dirac equation $i\hbar\partial_t\psi = \hat{H}\psi$, with

$$\hat{H} = mc^2\underline{\beta} + \hat{H}_0 + qV - c\sum_{i=1}^{3}(\hat{p}_i - qA_i)\underline{\alpha}_i. \tag{7}$$

The 4×4 matrices $\underline{\beta}$ and $\underline{\alpha}_i$ take their standard form [15]. The initial state can still be expanded as in Eq. (1), with $\phi_p(z)$ replaced by spinor momentum eigenstates $\phi_p^{(r)}(z) = \exp(ipz/\hbar)\,\theta^{(r)}(p)$, where

$$\theta^{(1)}(p) = \frac{1}{\sqrt{2}}\left[\sqrt{1+\frac{m}{E}},0,\frac{p}{\sqrt{E(m+E)}},0\right], \tag{8}$$

$$\theta^{(2)}(p) = \frac{1}{\sqrt{2}}\left[0,\sqrt{1+\frac{m}{E}},0,\frac{-p}{\sqrt{E(m+E)}}\right], \tag{9}$$

$$\theta^{(3)}(p) = \frac{1}{\sqrt{2}}\left[\sqrt{1-\frac{m}{E}},0,-\frac{p}{\sqrt{E(E-m)}},0\right], \tag{10}$$

$$\theta^{(4)}(p) = \frac{1}{\sqrt{2}}\left[0,\sqrt{1-\frac{m}{E}},0,\frac{p}{\sqrt{E(E-m)}}\right], \tag{11}$$

with the relativistic energy $E(p) = \sqrt{p^2c^2 + m^2c^4}$. Using this expression for $E(p)$, the free evolution rule (ii) can also be used for relativistic electrons.

To see that the acceleration rule (iii) can still be applied, we have to solve the Dirac equation with constant acceleration a [16–21], corresponding to $A_i = 0$ and $qV = -maz$ in Eq. (7). To keep a close analogy to the nonrelativistic treatment of Ref. [13], we expand the wave function as

$$\psi(z,t) = \sum_{r=1}^{4}\tilde{\psi}_r(t)\phi_{p(t)}^{(r)}(z), \tag{12}$$

with $p(t) = p + mat$. Inserting this into the Dirac equation and exploiting the orthonormality of the spinors $\theta^{(r)}(p)$, we obtain

$$i\partial_t\tilde{\psi}_r = \epsilon_r\frac{E(p(t))}{\hbar}\tilde{\psi}_r - i\epsilon_r(-1)^r\eta(t)\tilde{\psi}_{r+2\epsilon_r}, \tag{13}$$

with

$$\eta(t) \equiv \frac{a}{2c}\left[\frac{mc^2}{E(p(t))}\right]^2, \tag{14}$$

and $\epsilon_r = 1(-1)$ for $r = 1,2$ (3,4), respectively. $\eta(t)$ describes a coupling between positive- and negative-energy solutions that is maximal for $E(p(t)) \approx mc^2$. For constant values of η and $E(p)$, we find that the maximal transition probability is given by $\hbar^2\eta^2/[E(p)^2 + \hbar^2\eta^2]$, which is only significant for extreme accelerations of $a \approx 10^{30}$ m/s^2 or larger. For realistic accelerations, $\eta(t)$ is negligible, so that the solution to the accelerated Dirac equation can be approximated by

$$\tilde{\psi}_r(t) \approx e^{-\frac{i}{\hbar}\epsilon_r \int_0^t dt' E(p(t'))}\tilde{\psi}_r(0). \tag{15}$$

Consequently, Eq. (2) can also be used to describe the accelerated evolution of relativistic electron wave packets.

In Sec. IV, it will be shown that beam-splitting rule (iv) also applies to relativistic electrons if specific conditions are met. Hence, with the appropriate replacements, rules (i)–(iv) and, hence, final state (6) are still valid for relativistic electrons. Compared to Ref. [13], we have admitted that the time $\tilde{T}$ between the last two pulses, and the momentum transfer $2\hbar\tilde{k}_L$ in the electron rest frame, differ from the respective values for the first two pulses. A factor of γ appears in Eq. (6), which is formulated in the laboratory frame, because we have to perform a Lorentz transformation of the momentum transfer to obtain the momentum transfer in the laboratory frame.

In the nonrelativistic case, it is possible to evaluate Eq. (6) analytically for a Gaussian initial wave packet of spatial width w, for which

$$\tilde{\psi}(p) = \sqrt{\sqrt{\frac{2}{\pi}}\frac{w}{\hbar}}e^{-p^2w^2/\hbar^2}. \tag{16}$$

In the relativistic case, we can obtain an approximate solution by exploiting that the momentum width of the wave packets is still small after the acceleration. We can, therefore, expand all exponentials to second order in p and replace the spinor $\theta^{(r)}(p + maT')$ by $\theta^{(r)}(maT')$. Then all integrals in Eq. (6) are of Gaussian form and can be solved analytically, leading to partial beams with a Gaussian spatial structure. The final mean positions of the two partial beams in the laboratory frame evaluate to

$$z_{\mathrm{A}} = \Delta z + \frac{c^2}{a}(\gamma - 1) + \tilde{T}\left(\beta c - \frac{1}{\gamma^2}\frac{2\hbar\tilde{k}_L}{m}\right), \tag{17}$$

$$z_{\mathrm{B}} = \frac{c^2}{a}(\gamma - 1) + \tilde{T}\beta c, \tag{18}$$

where we have used $\Delta z = T\Delta v = 2T\hbar k_L/m$ for the separation induced by the first pair of laser pulses. These mean positions agree with relativistic trajectories of classical point particles in the laboratory frame. $c^2(\gamma - 1)/a$ corresponds to the distance traveled by the electrons during the acceleration phase. For $\gamma = 5/4$ and an acceleration of 1.8×10^{16} m/s^2, which corresponds to an electric-field strength of 10^5 V/m, this distance is about 1.3 m.

Terms proportional to $\tilde{T}$ correspond to the distance traveled by the partial beams between the last two laser pulses. βc is the velocity of electrons with momentum $p = m\gamma\beta c$, which have not received a momentum kick. Electrons that have received a momentum kick $\Delta\tilde{p} = -2\hbar\tilde{k}_L$ in their rest frame possess a momentum $p + \gamma\Delta\tilde{p}$ in the laboratory frame. The relativistic relation between velocity and momentum is given by $\beta(p) = p/\sqrt{p^2 + m^2c^2}$. Expanding $\beta(p + \gamma\Delta\tilde{p})$ to first order in $\Delta\tilde{p}$ produces the terms proportional to $\tilde{T}$ in Eq. (17).

To realize the proposal presented in Sec. II, $\tilde{T}$ has to be chosen in such a way that the distance between beams A and B is reduced by an amount Δz between the last two laser pulses. If $\Delta\tilde{v} = 2\hbar\tilde{k}_L/m$ denotes the relative velocity of the two partial beams in their rest frame, the proper time needed to cover this distance is given by $\tau = \Delta z/\Delta\tilde{v}$. In the laboratory frame, the time between the two pulses must therefore be chosen as $\tilde{T} = \gamma\tau = \gamma\Delta z\, m/(2\hbar\tilde{k}_L)$. The final distance between the two beams in the laboratory frame is then given by $z_{\mathrm{A}} - z_{\mathrm{B}} = \Delta z(1 - \gamma^{-1})$. Lorentz contraction implies that in the rest frame of the electrons, the distance is then given by $\gamma(z_{\mathrm{A}} - z_{\mathrm{B}}) = (\gamma - 1)\Delta z$, which corresponds to the mismatch discussed in Sec. II.

IV. KAPITZA-DIRAC BEAM SPLITTER FOR RELATIVISTIC ELECTRONS

The analysis given in Sec. III employs rule (iv), which has been derived for nonrelativistic electrons [13] using a modified Kapitza-Dirac effect and is only correct in the limit of very short laser pulses. Rule (iv) is sufficient to give a rough description of the interaction of electrons with the first two laser pulses, but it needs to be reconsidered for relativistic electrons interacting with the two laser pulses after the acceleration. The relativistic Kapitza-Dirac effect has been studied in Ref. [22]. To describe the modified relativistic Kapitza-Dirac effect for each of the four pulses, we need to solve the Dirac equation (7) in the presence of two counterpropagating laser fields with different frequencies. The corresponding electromagnetic potentials are given by $V = 0$ and $\vec{A} = \vec{\epsilon}(A^{(+)} + A^{(-)})$, where

$$A^{(+)} = -\frac{iE_1 e^{ik_1 z - it\omega_1 + i\theta_1}}{4\omega_1} - \frac{iE_2 e^{-ik_2 z - it\omega_2 + i\theta_2}}{4\omega_2} \tag{19}$$

is the positive-frequency part of the vector potential in the laboratory frame and $A^{(-)} = (A^{(+)})^*$. E_i and ω_i ($i = 1,2$) are electric-field amplitude and frequency of the two counterpropagating fields and $k_i = \omega_i/c$ is their wave number. The unit vector $\vec{\epsilon}$ describes the polarization direction in the x-y plane and θ_i are phase factors.

For nonrelativistic velocities, the Dirac equation can be solved using a Foldy-Wouthuysen transformation [15]. The large components of the Dirac spinor are then of the form $\psi = \exp(-imc^2t/\hbar)\tilde{\psi}$, where $\tilde{\psi}$ is a solution to the Schrödinger equation with the same vector potential. The analysis of Ref. [13] can therefore be applied to the first two laser pulses.

To describe the last two laser pulses, we can exploit that despite the relativistic mean electron velocity, the velocity spread is still nonrelativistic. We therefore can perform a Lorentz boost of the Dirac equation along the z axis into the (mean) electron rest frame. Because of the covariance of the Dirac equation, the result will still be of the form (7), but with a transformed vector potential.

The Lorentz transformation of the four-vector potential $(0,\vec{A})$ can be easily accomplished by noting that its polarization is perpendicular to the direction of the boost. Consequently, the vector potential still has the form (19), except that in the exponentials, we have to make the replacements $\omega_1 \rightarrow \tilde{\omega}_1 \equiv (1-\beta)\gamma\omega_1$ and $\omega_2 \rightarrow \tilde{\omega}_2 \equiv (1+\beta)\gamma\omega_2$. Therefore, detuning $\Delta\omega \equiv \omega_2 - \omega_1$ and average wave number $k_L \equiv (k_1 + k_2)/2$ in the laboratory frame need to be replaced by the respective values in the electron rest frame,

$$\Delta\tilde{\omega} = \gamma[\Delta\omega + \beta(\omega_2 + \omega_1)], \tag{20}$$

$$\tilde{k}_L = \frac{\gamma}{2c}[(1+\beta)\omega_2 + (1-\beta)\omega_1]. \tag{21}$$

It was shown in Ref. [13] that rule (iv) provides a reasonable approximation for the evolution of the electron state inside a bichromatic laser pulse if the resonance condition

$$\Delta\tilde{\omega} = \mp 2\frac{\hbar}{m}\tilde{k}_L^2 \tag{22}$$

is fulfilled. For relativistic electrons, this poses a practical limitation: because of the Doppler effect [terms proportional to β in Eq. (20)], the detuning $\Delta\tilde{\omega}$ in the electron rest frame may be very large. However, the Kapitza-Dirac effect requires phase locking, i.e., there must be a stable relation between the phases of the two counterpropagating laser fields [12]. In current experiments, such a relation can only be established for small detunings [23] or in harmonic generation [24]. We therefore propose the following setup: laser field 2 with frequency ω_2 is detuned by a small amount $\delta\omega$ from, and phase locked to, a pump laser of frequency $\omega_2 - \delta\omega$. Laser field 1 corresponds to the nth harmonic frequency of the pump laser, so that $\omega_1 = n(\omega_2 - \delta\omega)$. We then obtain

$$\Delta\tilde{\omega} = n(1-\beta)\gamma\delta\omega + [1+\beta - n(1-\beta)]\gamma\omega_2, \tag{23}$$

$$\tilde{k}_L = \frac{\gamma}{2c}\{[1+\beta + n(1-\beta)]\omega_2 - (1-\beta)\delta\omega\}. \tag{24}$$

If the final velocity of the electrons takes the value $\beta = (n-1)/(n+1)$, then these relations simplify to $\Delta\tilde{\omega} = \sqrt{n}\delta\omega$ and $\tilde{k}_L \approx \sqrt{n}\omega_2/c = \sqrt{n}k_2$. The resonance condition can then easily be fulfilled by choosing $\delta\omega = \mp 2\hbar\sqrt{n}k_2^2/m$, which apart from a factor of $\sqrt{n}$ is the same condition as in the nonrelativistic case. Hence, if the electrons are accelerated to a specific velocity, rule (iv) can still be used to describe the beam splitters.

V. NUMERICAL RESULTS

In Fig. 2, we show a full numerical simulation of the interference pattern, including the full Kapitza-Dirac effect as described in Ref. [13] instead of the simplified rule (iv). We assume fourth-order harmonic generation ($n = 4$), which corresponds to $\beta = 3/5$, so that electrons need to travel through an electric potential difference of 127.75 kV (see Fig. 1). The flight durations used in the simulation are $T = 50$ ns, $T' = 12.5$ ns, and $\tilde{T} = 31$ ns. The distance between wave packets A and B of about 15 μm corresponds to the spatial mismatch induced by Lorentz contraction. Wave packets with Roman numbers are labeled in the same way as in Ref. [13] and represent other partial beams.

The details of the numerical simulation are as follows. We performed all calculations in momentum space and used a grid of 10 000 points for a Fourier transformation of the final wave function to obtain the spatial density shown in Fig. 2.

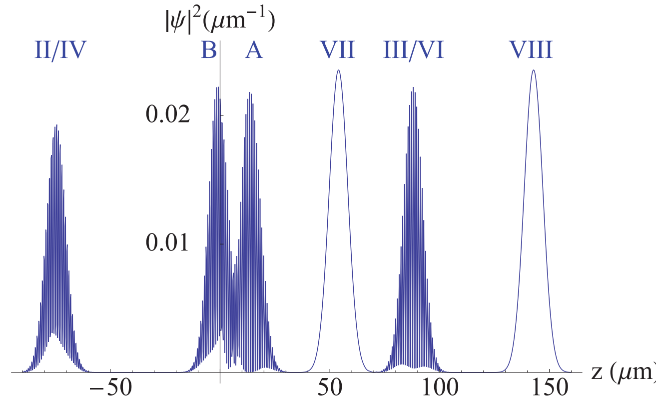

FIG. 2. (Color online) Numerical simulation of the split electron beam after the last laser pulse. The offset between beams A and B is a consequence of Lorentz contraction. See Sec. V for further details.

Rules (i) and (ii) can be evaluated exactly in momentum space. For the acceleration of 1.8×10^{16} m/s^2 that we considered, rule (iii) provides an excellent approximation and can also be evaluated directly. To implement an accurate description of rule (iv), we use the result that each bichromatic pulse couples a wave function with momentum p to wave functions with momentum $p \pm 2\hbar k_L$ [13]. As these momenta are coupled to other momenta, one obtains a coupling between an infinite set of momenta separated by multiples of $2\hbar k_L$. However, for a pulse duration of $t_L = \pi/(4g_1g_2) = 1.56$ ns, where g_i is defined in Eq. (7) of Ref. [13], the laser intensities are so low that this coupling is very weak and can be neglected except when resonance condition (22) [or Eq. (12) of Ref. [13] for nonrelativistic electrons] is fulfilled. We therefore only need to take into account the coupling between two resonant momenta, so that the unitary time evolution operator during a laser pulse can be found analytically by diagonalizing a 2×2 matrix. We remark that this procedure is more accurate than Eq. (5), which neglects the actual time evolution during the laser pulses and only describes how the electron momentum is changed.

The method presented in the preceding paragraph is nonrelativistic and provides an accurate description of the electron dynamics during the first two laser pulses. To apply this procedure to the last two laser pulses, we performed a Lorentz transformation of the numerical wave function at the end of the acceleration phase into the (mean) rest frame of the electrons in beam B, taking into account the changes to the vector potential discussed in Sec. IV. The evolution during the last two laser pulses and the free evolution between these pulses is then evaluated in the rest frame of beam B. Figure 2 shows the final wave function in this frame.

To check the numerical results, we have verified that the wave function is normalized and the mean position of all partial beams agrees with the position (in the rest frame of beam B) of a classical relativistic point particle that receives a specific momentum kick at each laser pulse. We remark that the distance between wave packets A and B in Fig. 2 is not exactly equal to the shift $(\gamma - 1)\Delta z$ derived in Sec. II, but is rather given by

$$z_A - z_B = (\gamma - 1)\Delta z + \gamma t_L \frac{2\hbar k_L}{m} - t_L \frac{2\hbar\tilde{k}_L}{m}. \tag{25}$$

The reason is that Eq. (25) takes into account the finite duration t_L of the laser pulses, while the discussion in Secs. II and III assumes that the momentum of the electrons changes instantaneously.

VI. BELL'S SPACESHIP PARADOX

Bell's spaceship paradox, which was popularized by Bell [25] but originally suggested by Dewan and Beran [26], is one of the thought experiments illustrating the subtleties of special relativity. Two spaceships are initially at rest and connected by a taut thread. They undergo the same acceleration until they reach relativistic speed. An observer in the laboratory frame would conclude that the thread will not break because the distance between the spaceships would never change. However, in the reference frame of the ships, Lorentz contraction would imply that the thread should break.

The paradox can be explained using the space-time diagram shown in Fig. 3. Blue solid lines describe the trajectories of two spaceships (A and B), which are initially separated by a distance Δz. They are accelerated until they reach relativistic speed. After the acceleration, an observer in the laboratory frame would measure the distance between the ships simultaneously in her frame, along the horizontal black dashed line in Fig. 3. She would conclude that the distance is still given by Δz, which is the proper distance between the end points of the black dashed line. An observer on a ship would measure the distance simultaneously in his frame, along the bold dashed red line in the figure. The reason for the change in the distance is the relativity of simultaneity. In the reference frame of ship A, ship B stopped to accelerate earlier and thus had more time to travel to the right.

To analyze the paradox, some authors use space-time diagrams only [27–30]. Other authors address the question of whether Lorentz contraction will cause stress forces in the string to occur, which may trigger the string to break and thus provide a physical signal that resolves the paradox. The answer to this question is much more involved due to the subtleties of relativistic rigid-body dynamics and has been addressed with different methods and results [25,26,31–36]. Most authors came to the conclusion that the string would break.

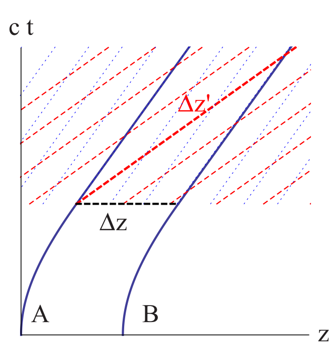

FIG. 3. (Color online) Space-time diagram of Bell's spaceship paradox. Solid blue lines correspond to the world line of the two ships. Dashed red lines (dotted blue lines) are the spatial (temporal) coordinate lines, respectively, in the reference frame of the spaceships after they were accelerated.

Comparing Figs. 1(b) and 3, one can see that Bell's paradox and the proposed interference experiment are closely related. Except for the parts in which electron beams A and B are split and recombined, the two space-time diagrams coincide. In both cases, it is Lorentz contraction of the final separation $\Delta z'$ that is responsible for a physical effect: the mismatch between the final positions of beams A and B in the electron interferometer and the breaking of the string in Bell's paradox. One may say that the mismatch in the interference experiment replaces the breaking of the string as a physical signature for the resolution of the paradox.

VII. DISCUSSION

The theoretical analysis that we have presented above is based on several simplifying assumptions, including a homogeneous electric field, laser pulses that are switched on and off at specific times, and a one-dimensional analysis that ignores forces in the x and y direction. In this section, we estimate how deviations from these assumptions may affect the proposed experiment. In doing so, it is important to keep the following points in mind:

(i) Strictly speaking, the proposed experiment is not an interference experiment. The measured quantity is a displacement between two partial beams, which would also be produced for incoherent electron beams. However, if the two partial beams are partially overlapping, the fringe visibility can provide information about the displacement. Coherence is therefore helpful but not essential.

(ii) The measured observable is a relative displacement of two partial beams along the direction of the laser pulses. Any effects that affect the motion in other directions, such as forces in the x or y direction, do not, therefore, affect the result. Similarly, forces in the z direction that affect both partial beams in the same way will not affect the displacement.

(iii) The beam-splitting process is velocity selective, i.e., the electron beam is only split or recombined for electrons within a specific velocity range.

With these remarks, we can address a number of experimentally relevant questions.

Pulse timing. In our theoretical analysis, the counterpropagating light pulses are switched on and off simultaneously everywhere in space. In reality, the pulses are propagating in opposite directions and will hit the fast-moving partial electron beams at different times. In the proposed setup, this is not a problem because only partial beam A actually interacts with the pulses, while partial beam B does not obtain a momentum transfer. In an experiment, pulse timing should therefore be designed in such a way that partial beam A interacts with the pulses at the correct time.

Pulse shape. The spatial shape of a light pulse also affects the force that light exerts on charged particles. Because of point (ii) above, the transverse pulse profile will not have a significant influence on the displacement between beams A and B. As a rule of thumb, the magnitude of the momentum change due to the envelope $\mathcal{E}$ of a pulse is much smaller than the momentum transfer in a resonant absorption or emission process, as long as the envelope changes slowly over the range of one wavelength λ, so that $\lambda|\nabla\mathcal{E}| \ll |\mathcal{E}|$ [37]. The transverse profile would therefore only generate a displacement in the

x-y plane that is much smaller than the displacement of partial beam VIII in Fig. 2. Similar remarks apply to the longitudinal pulse profile. However, the longitudinal profile must be shaped in such a way that the electron-pulse interaction is not switched on adiabatically [38].

Photon emission. It is well known that accelerated charges emit radiation. In matter-wave interferometry, even the emission of a single photon may lead to a loss of coherence [39]. While point (i) implies that this loss of coherence is not a fundamental problem, the associated change in the electron momentum may nevertheless affect the displacement between partial beams A and B. It is, therefore, worthwhile to estimate the probability of photon emission during the acceleration.

The photon emission probability for an accelerated electron per unit time and transverse momentum p_x, p_y is given by [40]

$$P(p_x, p_y) = \frac{q^2 c^2}{\pi^2 a \varepsilon_0 \hbar^3} \left| K_1\left(\frac{c^2}{\hbar a} \sqrt{p_x^2 + p_y^2} \right) \right|^2, \quad (26)$$

where K_1 denotes the modified Bessel function of the second kind. The total probability to emit a photon can then be estimated by

$$P_{\mathrm{em}} = T' \int dp_x\, dp_y\, P(p_x, p_y) \quad (27)$$

$$= 2\pi T' \int_0^\infty dk_\perp \frac{q^2 c^2}{\pi^2 a \varepsilon_0 \hbar} \left| K_1\left(\frac{c^2}{a} k_\perp \right) \right|^2, \quad (28)$$

with $k_\perp = \sqrt{p_x^2 + p_y^2}/\hbar$ the transverse wave number of the electron. This integral is logarithmically divergent for large wavelengths, $k_\perp \to 0$. We regularize it by replacing the lower boundary by $u\, a/c^2$, where $u > 0$ parametrizes the value of the cutoff and c^2/a corresponds to the maximal distance (the largest wavelength) that fits into a Rindler wedge [41] in the reference frame of an accelerated observer. The integral can then be performed numerically. For the parameters used in Sec. V, $P_{\mathrm{em}}(u)$ varies very slowly with u and is less than 5% for $u > 10^{-4}$. We therefore expect that photon emission will not pose a problem for the proposed experiment.

Spatial field fluctuations. In the previous sections, we have assumed that the electric field is homogeneous and time independent. Spatial homogeneity is not a critical assumption because it only matters that both partial beams achieve the same Lorentz factor γ at the end of the acceleration phase. Because both partial beams essentially follow the same path and are only separated along the z axis, both beams would undergo the same (nonconstant) acceleration before they are recombined. Hence, field fluctuations along the z axis would not affect the experimental outcome. Transverse field fluctuations in the x or y direction could result in different acceleration for both beams, but this would be accompanied by a displacement of the beams in the x-y plane. For a given point in the x-y plane, the z displacement should still be the same. The only spatial field fluctuations that would be of concern are those which couple transverse and longitudinal motion of the electrons. They can be dealt with in a similar way as temporal fluctuations (see below).

Temporal field fluctuations. To avoid electric forces between two partial beams, the experiment should be performed in such a way that only one electron passes through the interferometer in each run. Temporal fluctuations in the electric field could significantly change the dynamics of the electrons between different runs and thus make it impossible to measure the beam displacement. Fortunately, point (iii) provides a way to overcome this problem: only electrons that are at the right time, and with the correct velocity, at the location of the laser pulse will interact with it. Thus, the resonant interaction with laser pulses selects those electrons which have obtained the proper velocity and position to contribute to the measured observable.

In the setup shown in Fig. 1, velocity selection would only apply to partial beam A because beam B does not interact with the laser pulses. The setup could be modified in such a way that both beams A and B would receive a momentum transfer from (possibly different) laser pulses after the acceleration. In this way, both beams would be subject to velocity selection. Furthermore, such a modification could be used to move beams A and B away from background electrons that do not interact with the laser pulses, similarly to beam VIII in Fig. 2. A disadvantage of velocity selection is that runs in which an electron has the wrong velocity will not contribute to the measurement. The total number of experimental runs needed will therefore be increased.

Detection. To detect the interference pattern of electrons moving at relativistic speed, a time-of-flight measurement may be needed. Alternatively, it would be possible to decelerate the electrons after the last laser pulse and detect the electrons when they obtained nonrelativistic speed. Such a deceleration phase would lead to a Lorentz contraction of the distance between the two electron beams, but it would not undo the separation.

VIII. CONCLUSION

We have proposed an experiment in which Lorentz contraction changes the interference pattern in an electron interferometer. Two partial beams, which would be perfectly overlapping for nonrelativistic electrons, will miss each other by an amount $\Delta z(\gamma - 1)$, with Δz the beam separation in the interferometer. The experiment is closely related to Bell's spaceship paradox, with the mismatch of the beams replacing the breaking of a string as physical evidence for Lorentz contraction.

The key element of our proposal is the use of laser pulses to modify the electron motion via the Kapitza-Dirac effect. Using fields instead of gratings as beam splitters enables us to fix time and location of the splitting process in the rest frame of the electrons, rather than in the laboratory frame. In combination with the large accelerations that can be achieved for charged elementary particles in general, this method may pave the way to further tests of relativity, such as local Lorentz invariance [42] or extended relativity [43].

ACKNOWLEDGMENTS

This project was funded by NSERC, ACEnet, and UCR of St. Francis Xavier University. We thank J. Franklin for comments on a previous version of the manuscript.

[1] C. Bordé, Phys. Lett. A **140**, 10 (1989).
[2] C. J. Bordé, C. Salomon, S. Avrillier, A. Van Lerberghe, C. Bréant, D. Bassi, and G. Scoles, Phys. Rev. A **30**, 1836 (1984).
[3] J. D. Bjorken, Phys. Rev. D **27**, 140 (1983).
[4] G. Margaritondo and P. Rebernik Ribic, J. Synch. Rad. **18**, 101 (2011).
[5] J. Levy, arXiv:physics/0603267 [physics.gen-ph].
[6] F. Riehle, T. Kisters, A. Witte, J. Helmcke, and C. J. Bordé, Phys. Rev. Lett. **67**, 177 (1991).
[7] J. Audretsch and K.-P. Marzlin, Phys. Rev. A **47**, 4441 (1993).
[8] J. Audretsch and K.-P. Marzlin, Phys. Rev. A **50**, 2080 (1994).
[9] P. L. Kapitza and P. A. M. Dirac, Math. Proc. Camb. Phil. Soc. **29**, 297 (1933).
[10] H. Batelaan, Rev. Mod. Phys. **79**, 929 (2007).
[11] P. H. Bucksbaum, D. W. Schumacher, and M. Bashkansky, Phys. Rev. Lett. **61**, 1182 (1988).
[12] D. L. Freimund, K. Aflatooni, and H. Batelaan, Nature (London) **413**, 142 (2001).
[13] K.-P. Marzlin, Phys. Rev. A **88**, 043621 (2013).
[14] D. L. Freimund, Ph.D. thesis, University of Nebraska, 2003.
[15] J. D. Bjorken and S. D. Drell, *Relativistic Quantum Mechanics* (McGraw-Hill, New York, 1998).
[16] M. Soffel, B. Müller, and W. Greiner, Phys. Rev. D **22**, 1935 (1980).
[17] F. W. Hehl and W.-T. Ni, Phys. Rev. D **42**, 2045 (1990).
[18] F. Domínguez-Adame and M. A. González, Europhys. Lett. **13**, 193 (1990).
[19] R. Jáuregui, M. Torres, and S. Hacyan, Phys. Rev. D **43**, 3979 (1991).
[20] P. M. Alsing, I. Fuentes-Schuller, R. B. Mann, and T. E. Tessier, Phys. Rev. A **74**, 032326 (2006).
[21] Y. Ling, S. He, W. Qiu, and H. Zhang, J. Phys. A **40**, 9025 (2007).
[22] S. Ahrens, H. Bauke, C. H. Keitel, and C. Müller, Phys. Rev. Lett. **109**, 043601 (2012).
[23] J. Appel, A. MacRae, and A. I. Lvovsky, Meas. Sci. Technol. **20**, 055302 (2009).
[24] R. Zerne, C. Altucci, M. Bellini, M. B. Gaarde, T. W. Hänsch, A. L'Huillier, C. Lyngå, and C.-G. Wahlström, Phys. Rev. Lett. **79**, 1006 (1997).
[25] J. S. Bell, *Speakable and Unspeakable in Quantum Mechanics* (Cambridge University Press, Cambridge, UK, 2004).
[26] E. Dewan and M. Beran, Am. J. Phys. **27**, 517 (1959).
[27] A. A. Evett, Am. J. Phys. **40**, 1170 (1972).
[28] F. J. Flores, Phys. Educ. **40**, 500 (2005).
[29] D. V. Redžić, Europ. J. Phys. **29**, N11 (2008).
[30] T. Matsuda and A. Kinoshita, AAPPS Bull. **14**, 3 (2004).
[31] P. J. Nawrocki, Am. J. Phys. **30**, 771 (1962).
[32] E. M. Dewan, Am. J. Phys. **31**, 383 (1963).
[33] D. T. Cornwell, Europhys. Lett. **71**, 699 (2005).
[34] J. Franklin, Eur. J. Phys. **31**, 291 (2010).
[35] A. Tartaglia and M. L. Ruggiero, Europ. J. Phys. **24**, 215 (2003).
[36] D. F. Styer, Am. J. Phys. **75**, 805 (2007).
[37] H. Wallis, Phys. Rep. **255**, 203 (1995).
[38] M. Fedorov, Opt. Commun. **12**, 205 (1974).
[39] T. Pfau, S. Spälter, C. Kurtsiefer, C. R. Ekstrom, and J. Mlynek, Phys. Rev. Lett. **73**, 1223 (1994).
[40] A. Higuchi, G. E. A. Matsas, and D. Sudarsky, Phys. Rev. D **46**, 3450 (1992).
[41] N. D. Birrell and P. C. W. Davies, *Quantum Fields in Curved Space* (Cambridge University Press, Cambridge, UK, 1984).
[42] I. Vetharaniam and G. E. Stedman, Class. Quant. Grav. **11**, 1069 (1994).
[43] Y. Friedman and Y. Gofman, Phys. Scr. **82**, 015004 (2010).